Journal of Materials Chemistry A

Poly(norbornene) Anion Conductive Membranes: Homopolymer, Block Copolymer and Random Copolymer Properties and Performance

Journal:	*Journal of Materials Chemistry A*
Manuscript ID	TA-ART-05-2020-004756.R1
Article Type:	Paper
Date Submitted by the Author:	27-Jul-2020
Complete List of Authors:	Mandal, Mrinmay; Georgia Institute of Technology, School of Chemical and Biomolecular engineering Huang, Garrett; Georgia Institute of Technology Hassan, Noor; University of South Carolina Mustain, William; University of South Carolina System, Chemical Engineering; University of South Carolina System, Kohl, Paul; georiga tech; Georgia Institute of Technology,

Poly(norbornene) Anion Conductive Membranes: Homopolymer, Block Copolymer and Random Copolymer Properties and Performance

Mrinmay Mandal,[1] Garrett Huang,[1] Noor Ul Hassan[2], William E. Mustain[2], and Paul A. Kohl[*1]

[1]School of Chemical and Biomolecular Engineering, Georgia Institute of Technology, Atlanta, GA

[2]Department of Chemical Engineering, University of South Carolina, Columbia, SC

Keywords: anion exchange membranes (AEMs), vinyl addition, poly(norbornene), cross-linking, homopolymer, random copolymer, block copolymer.

* Contact author: kohl@gatech.edu, 404-894-2893

Abstract

It has previously been shown that phase-separated block copolymers with non-ion conducting (hydrophobic) blocks and ion conducting (hydrophilic) blocks can form efficient ion conducting channels with high ionic mobility and conductivity. Block copolymers can provide a means for phase segregation and ion channel formation while homopolymers and random copolymers have been shown to have lower ion mobility. In this study, the properties of poly(norbornene) based anion exchange membranes (AEMs) comprising homopolymers, block copolymers, and random copolymers with high ion-exchange capacity (IEC) (3.48-4.55 meq/g) have been investigated and compared. The polymers were cross-linked with *N*,*N*,*N*′,*N*′-tetramethyl-1,6-hexanediamine before casting the membranes to avoid excessive water swelling due to high water uptake. It was shown that high ionic conductivity can be achieved in both random copolymers and homopolymers even in the absence of microphase-separated structures. For example, the conductivity of a random copolymer was 194 mS/cm at 80 ºC, which was comparable to the block copolymer, 201 mS/cm at 80 ºC. The H_2/O_2 fuel cell performance of random copolymer composite membranes showed a peak power density of 3.05 W/cm^2 and peak current density of 7.85 A/cm^2 at 80 °C compared to block copolymer membranes (peak power density of 3.21 W/cm^2 and peak current density of 8.27 A/cm^2 at 80 °C). It is more critical that high water transport be achieved in AEMs than achieving a phase-segregated morphology. Finally, the homopolymer, block copolymer, and random copolymer membranes showed <1.35% degradation after aging in 1 M NaOH at 80 °C for 1000 h.

Introduction

Anion exchange membranes (AEMs) have attracted attention as a replacement to high-cost proton exchange membranes (PEMs). AEMs are widely used in electrochemical devices such as fuel cells, electrolyzers, electrochemical separations, and redox flow batteries.[1-4] When used in electrochemical devices, the benefits of high pH AEMs compared to low pH PEMs include the use of non-precious catalysts, facile oxygen reaction kinetics, and reduced fuel crossover.[5-8] However, it is important to have AEMs which are mechanically robust so that thin, highly conductive membranes with excellent chemical stability can be realized.[9] Several recent reports have demonstrated membranes that have acceptable ionic conductivity, ex-situ chemical stability at high pH, and low/moderate water uptake (WU).[10-15]

The positive properties of poly(norbornene) multi-block copolymers (BCP) with an all-hydrocarbon backbone and long-tail tethered cations, allowing for high device performance in anion exchange membrane fuel cells (AEMFCs), have been reported.[16,17] The BCP architecture contributed to high ion mobility. These membranes have enabled a very high AEMFC peak power density of 3.5 W/cm^2 (80 °C with H_2/O_2) to be achieved.[16] Polynorbornene anion conducting ionomers were also used in direct borohydride fuel cells (DBFCs) using alkaline $NaBH_4$ fuel feed and H_2O_2 as the oxidant.[18] By attaching the cation via a long alkyl side-chain for anion conduction, two primary AEM degradation mechanisms, S_N2 substitution and Hoffmann elimination, are avoided.[19-22]

Water management is an important aspect of electrochemical devices for achieving high performance, such as in AEM fuel cells (AEMFC).[16,23-26] Water is present in the form of bound water of hydration (productive) and unbound, free (sometimes unproductive) water molecules inside the membrane. Bound water and limited amounts of unbound water help in the hydration and transport of mobile anions. However, excess free water reduces ion mobility and causes mechanical failure by swelling and softening the membrane due to the flooding of the ion conductive channel. Hence, it is necessary to avoid water imbalance without degrading other properties to enable high AEMFC performance. High water mobility and thin, robust membrane design in AEMFCs help the water distribution and transport during device operation.[16,17,26] In AEMFCs, water is electrochemically produced at the hydrogen anode during the hydrogen oxidation reaction (HOR) and consumed at the oxygen cathode by oxygen reduction reaction (ORR). Four water molecules are generated at the anode while, only two water molecules are

consumed at the cathode during the four-electron transfer.[26] Water also moves from the cathode to the anode during operation by electro-osmotic drag. Hence, anode flooding can occur at the hydrogen anode during operation. Another concern is that the local hydration number within the oxygen cathode can drop if insufficient water is present, which is more likely to happen at high current density when the water consumption rate is high. Dry out at the cathode can be mitigated by high internal water flux via diffusion from the hydrogen anode to the oxygen cathode across the membrane.[16] A detailed study using different thickness membranes led to a performance increase when thinner membranes were used enabling high water transport through the membranes.[16] The importance of water transport through the AEM has also been shown computationally[25]. One possible downside when creating AEMs with high water flux can be excessive WU and swelling. Light polymer cross-linking is an effective strategy to control WU in high IEC membranes without degrading transport within the membrane or the mechanical properties of the membrane.[16] For example, GT82-XX AEMs showed that WU decreased from 122% to 61% (which is a favorable change) when the cross-linker (TMHDA) concentration increased from 5 mol% to 20 mol% with respect to the available cross-linkable sites.[16] The IEC drop was marginal (from 3.82 to 3.72 meq/g due to the mass of the TMHDA) with the higher TMHDA concentration. Membranes with a low (5 mol%) TMHDA content were more susceptible to mechanical deformation. It is well known that the AEMs have poor ion mobility but higher mechanical properties when the membranes are cast with a high degree of cross-linking.[14,17]

The properties of poly(norbornene) AEM homopolymer, block copolymer, and random copolymer with high IECs were investigated in this study. Polymers were crossed-linked to limit excessive WU in order to avoid membrane softening. It is shown that water management is a more important factor than the phase-segregated morphology in determining the membrane properties and electrochemical device performance. It is shown that in this polymer system, nearly comparable conductivity was obtained for the random and BCP polymer membranes (194 mS/cm for random copolymer at 80 ºC and 201 mS/cm for block copolymer at 80 ºC), contrary to previous wisdom. The formation of very thin, mechanically flexible membranes with efficient water transport for high performance fuel cells was demonstrated. The random and block copolymer composite membranes had H_2/O_2 fuel cell performance of peak power density 3.05

W/cm^2 and 3.21 W/cm^2, respectively, and current density of 7.85 A/cm^2 and 8.27 A/cm^2, respectively, at 80 °C.

Experimental

Materials: The monomers, butyl norbornene (BuNB), bromobutyl norbornene (BBNB) and bromopropyl norbornene (BPNB), were supplied by Promerus, LLC (Brecksville, OH). Prior to polymerization, the monomers were purified by distillation over sodium and degassed in three freeze-pump-thaw cycles. The procedures were carried out in a dry argon atmosphere glove box with rigorous exclusion of moisture and air. The catalyst [(allyl)palladium(triisopropylphosphine)chloride, (η^3-allyl)Pd(^{i}Pr$_3$P)Cl)] was prepared following a previously published procedure.[27] Lithium tetrakis(pentafluorophenyl)-borate·(2.5Et$_2$O) (Li[FABA]) was purchased from Boulder Scientific Co. and used as received. *N*,*N*,*N*′,*N*′-Tetramethyl-1,6-hexanediamine (TMHDA), anhydrous toluene (99.9 %), anhydrous *α*,*α*,*α*-trifluorotoluene (TFT, ≥ 99 %) and tetrahydrofuran (THF) were purchased from Sigma-Aldrich and used as received.

Homopolymer, block copolymer, and random copolymer synthesis and characterization: The tetrablock copolymer (GT75, polymer containing 75 mol% of the halogenated monomer), homopolymer (GT100, polymer with 100 mol% of the halogenated monomer), and random copolymer (GTR75, polymer containing 75 mol% of the halogenated monomer) were synthesized following a previously reported procedure using bromobutyl norbornene (BBNB) and bromopropyl norbornene (BPNB).[13,14,28]

The materials for the random copolymer were synthesized in a nitrogen filled glove box. The catalyst solution was prepared by mixing (η^3-allyl)Pd(^{i}Pr$_3$P)Cl) and lithium tetrakis(pentafluorophenyl)-borate·(2.5Et$_2$O) (Li[FABA]) in 1: 1 mole ratio. A mixture of toluene and trifluorotoluene (TFT) was used as the solvent and the mixture was stirred for 20 min to generate the cationic Pd catalyst for polymerization. The monomers, butyl norbornene (BuNB) and bromobutyl norbornene (BBNB), were mixed together in a round-bottomed flask and purified through three freeze-pump-thaw cycles. Next, toluene was added to make a 5wt% solution of the monomer. The monomer solution using toluene as the solvent was added dropwise (10 s per drop) to the catalyst solution and stirred vigorously using a dropping funnel. After the addition was complete, the reaction mixture was and precipitated into methanol three

times. The resulting polymer was dissolved in THF and stirred over activated charcoal. The solution was passed through an alumina filter to remove palladium catalyst residue. The resulting product was precipitated from THF by addition of methanol. The polymer product was dried under vacuum at 60 °C. The homopolymer was synthesized from bromopropyl norbornene (BPNB) in a nitrogen filled glove box. The catalyst solution was prepared as described above. BPNB was purified through three freeze-pump-thaw cycles and toluene was added to make a 5 wt% solution of the monomer. The catalyst solution was injected at once into the monomer solution under vigorous stirring. After the polymerization was complete, the solid polymer was precipitated out of solution following the same procedure described above.

The polymer samples were analyzed by ^{1}H NMR using a Bruker Avance 400 MHz NMR instrument using $CDCl_3$ as the solvent. The number average molecular weight (M_n) and dispersity (Đ) of GT100, GT75, and GTR75 were determined by gel permeation chromatography (GPC) (Shimadzu) equipped with an LC-20 AD HPLC pump and a refractive index detector (RID-20 A, 120 V). GPC measurements were performed in THF with the eluent flow rate of 1.0 mL/min at 30°C and calibrated against a polystyrene standard.

Membrane characterization: In this study, 50 μm thick membranes were made for measuring the polymer (with TMHDA) properties. For fuel cell testing, ca. 10 μm thick reinforced composite membranes were cast. The reinforcement material was a microporous PTFE material. A detailed procedure for casting the membranes/composite membranes has been provided in an earlier report.[16] After casting, all membranes were soaked in a 50 *wt*% aqueous trimethylamine solution for 48 h at room temperature to convert the bromobutyl/bromopropyl moieties to quaternary ammonium head-groups. The quaternized membranes were ion-exchanged from bromide ions to hydroxide ions by immersion in 1 M NaOH solution under nitrogen for 24 h.

The ionic conductivity of the membranes was measured using four-point probe electrochemical impedance spectroscopy (1 Hz to 1 MHz) with a PAR 2273 potentiostat. The membranes were cut into 1 × 4 cm strips and tested in HPLC-grade water under a nitrogen purge to minimize carbonation. The membranes were allowed to equilibrate for 30 min prior to each measurement. The in-plane ionic conductivity was calculated using Equation 1.

$$\sigma = \frac{L}{WtR} \quad (1)$$

In Eq. 1, σ is the ionic conductivity, L is the length between the sensing electrodes, W and t are the width and thickness of the membranes, respectively, and R is the measured resistance. The long-term (>1000 h) alkaline stability test was performed by periodically measuring the ionic conductivity after soaking the membranes in hydroxide-form in aqueous 1 M NaOH at 80 °C in a Teflon-lined Parr reactor. Prior to each measurement, the membranes were taken out of solution and thoroughly washed with DI water. After each measurement, the membranes were stored in the reactors with fresh NaOH solution. After equilibration, each data point was measured in triplicate and the average value is reported here. The deviation in the value of each data point was <0.5%.

The ion-exchange capacities (IEC) of the precursor polymers were determined by ^{1}H NMR. Mohr's titration method was used to measure the IEC of the membranes after cross-linking and quaternization to confirm the accuracy of the NMR results.[29] In a typical procedure, the polymer in Br^- form was converted to Cl^- form by soaking in 0.1 M NaCl solution for 24 h. The film was removed from the NaCl solution, thoroughly washed with DI water and dried in vacuum for >24 h. The dry film weight was recorded. Next, the membranes were immersed in a fixed volume of 0.05 M $NaNO_3$ for 24 h. Finally, the released Cl^- was titrated with 0.05M $AgNO_3$ using K_2CrO_4 (10 wt%) as the indicator. Measurements were performed in triplicate to ensure repeatability. The deviation in the measurements of each data point was <1%. The IEC was calculated using Equation 2.

$$\mathrm{IEC} = \frac{\mathrm{C_{AgNO_3}} \times \mathrm{V_{AgNO_3}}}{\mathrm{M_d}} \quad (2)$$

In Eq. 2, V_{AgNO_3} (mL) is the volume of $AgNO_3$ solution, C_{AgNO_3} (0.05 mol·L^{-1}) is the concentration of $AgNO_3$ solution, and M_d (g) is the weight of the dried sample.

The percent swelling was calculated using Equation 3, where V_d is dry volume of the membrane and V_w is the volume of the fully hydrated membrane after removing excess surface water.

$$Swelling\ (\%) = \frac{V_w - V_d}{V_d} \times 100 \quad (3)$$

The WU was calculated using Equation 4.

$$\mathrm{WU}(\%) = \frac{\mathrm{M_w} - \mathrm{M_d}}{\mathrm{M_d}} \times 100 \quad (4)$$

In Eq. 4, M_d is the dry mass of the film and M_w is the wet mass of the film after removing excess surface water. The mass of the membranes was measured at room temperature in OH^- form. The hydration number (λ) or the number of water molecules per ionic group was calculated using Equation 5.

$$\lambda = \frac{1000 \times WU\%}{IEC \times 18} \quad (5)$$

The number of freezable water (N_{free}) and bound water (or non-freezable water) (N_{bound}) was determined by differential scanning calorimetry (DSC). DSC measurements were carried out on a Discovery DSC with an autosampler (TA Instruments). The samples were fully hydrated by soaking in deionized water for one week. After excess water on the surface was removed, a 5 to 10 mg sample was quickly cut and sealed in an aluminum DSC pan. The sample was first cooled to -70 °C at 5 °C/min and then heated to 30 °C at 5 °C/min under N_2 (20 mL/min). The quantity of freezable and non-freezable water was determined by Equations 6 to 8.[30-32]

$$N_{free} = \frac{M_{free}}{M_{tot}} \times \lambda \quad (6)$$

M_{free} is the mass of freezable water and M_{tot} is the total mass of water absorbed in the film. The weight fraction of freezable water was calculated using Equation 7.

$$\frac{M_{free}}{M_{tot}} = \frac{H_f/H_{ice}}{(M_W - M_d)/M_w} \quad (7)$$

M_w is the wet mass of the film obtained after gently wiping excess water from the surface. M_d is the dry mass of the film. H_f is the enthalpy obtained by the integration of the DSC freezing peak and H_{ice} is the enthalpy of water fusion, corrected for the subzero freezing point according to Equation 8.

$$H_{ice} = H^o_{ice} - \Delta C_p \Delta T_f \quad (8)$$

ΔC_p is the difference between the specific heat capacity of liquid water and ice. ΔT_f is the freezing point depression.

Small angle X-ray scattering (SAXS) was used to study the nanophase separation in the AEMs. Hydrated membranes in bromide form were tested in air using either the SAXSess mc^2 (Anton Paar) at the Center for Nanophase Materials Sciences (Oak Ridge National Laboratory, Oak Ridge, TN) or the NSLS-II beamline at the Center for Functional Nanomaterials

(Brookhaven National Laboratory, Upton, NY). The characteristic Bragg separation length or inter-domain spacing (d) was calculated using Equation 9.

$$d = \frac{2\pi}{q} \tag{9}$$

The storage modulus of the membranes was measured by dynamic mechanical analysis (DMA) using a TA Instruments Q800 under a 1 Hz single-frequency strain mode in air at 25 °C. A fully hydrated, rectangular sample was loaded into the DMA with tension clamps after removing surface water. Experiential parameters for the DMA were set to 0.1% strain and a preload force of 0.01 N with a force track of 125%.

Fuel cell testing: Gas diffusion electrodes (GDEs) were fabricated by spraying a catalyst ink made from polynorbonene tetrablock copolymer powder ionomers (GT32 and GT73) and Pt-based electrocatalysts onto Toray TGP-H-060 gas diffusion layers (GDLs) with 5% PTFE. Commercially available 40% Pt/C (Alfa Aesar HiSPEC 4000, Pt nominally 40%wt, supported on Vulcan XC-72R carbon) was used at the cathode and 60% Pt-Ru/C (Alfa Aesar HiSPEC 10000, Pt nominally 40 wt%., and Ru, nominally 20 wt%., supported on Vulcan XC-72R carbon) was used as the anode. The detailed procedure for ink formulation and GDE fabrication has been previously reported, though a brief description is provided below.[23,24,33]

To make the anode GDEs, the ionomer powder was ground with a mortar and pestle for 10 min to lower the particle aggregation. Then, the PtRu/C catalyst, and additional carbon (Vulcan XC-72R) were added to yield the following mass ionomer:carbon:catalyst mass ratio – 1:2.5:1.5. Next, 1 ml of DI water was added and the components were hand-ground with the mortar and pestle for an additional 10 minutes to yield a visually and texturally homogenous slurry. Two mL of isopropyl alcohol was added to the mortar and ground for 5 min, after which the catalyst slurry and combined with an additional 7 mL of 2-propanol to produce a low viscosity ink. PTFE (DUPONT ZONYL® Fluoroadditive Polytetrafluoroethylene Type MP1200) dispersion was added to the anode ink such that the PTFE would comprise 8% of the total catalyst layer mass. Each ink was homogenized in an ambient temperature ultrasonic bath (Fisher Scientific FS30H) for 60 min, during which time a mixture of ice and water was added to the ultrasonic bath to maintain the temperature at less than 20 °C. To make the cathode GDEs, the same procedure was followed as the anode except that the catalyst was Pt/C and no PTFE was added to the catalyst ink. The ionomer:carbon:Pt mass ratio was maintained at 1:2.5:1.5.

The catalyst inks were used to fabricate GDEs by hand-spraying the ink onto a larger area (25 cm^2) GDL with an Iwata Eclipse HP-CS spray gun using 12 to 15 psig N_2 (Airgas Ultra High Purity) carrier gas. Finally, 5 cm^2 GDEs were cut from the larger sprayed electrodes for use in the cell hardware. The catalyst loading for the anode was 0.7±0.03 mg(Pt/Ru)/cm^2 and for cathode was 0.6±0.02 mg(Pt)/cm^2.

Anion Exchange Membrane Fuel Cells (AEMFCs) with a 5 cm^2 active area were assembled by placing the anode and cathode GDEs on opposite sides of the AEM in Scribner fuel cell hardware with a single channel serpentine flow field. The GDEs were readied for cell use by convert them to the OH^- form through soaking in 1 M KOH solution for one hour, replacing the solution every 20 minutes. This was also done to the AEM. Excess KOH was completely removed from the surface of membrane and GDEs before assembly. Following pretreatment, the AEM was sandwiched between the anode and cathode GDEs (without any prior hot pressing) and the cell was torqued to 45 in.lb. 150 μm thick teflon sheets were cut to size and used as the cell gaskets for insulation and to prevent leakage of reactant gases. A Scribner 850e fuel cell test station was used to perform the fuel cell experiments and data collection. Fully humidified Nitrogen gas (N_2) was flowed through the anode and cathode at the cell startup with a cell temperature setting of 60 °C. After the set temperature is reached, the N_2 feeds were switched to Ultra High Purity (UHP) Hydrogen and Oxygen and a constant voltage of 0.6 V was applied as the break-in cell voltage. After a stable current density was established, the dew points of the anode and cathode reacting gases were optimized. The cell temperature was gradually increased to 80 °C in 5 °C increments, with the anode/cathode dew points being simultaneously optimized with the cell temperature to avoid membrane dry out. It is pertinent to mention that no backpressure is applied while testing the cell on H_2/O_2 feed. In our typical procedure, polarization and power density curves were collected by slowly sweeping the voltage from open circuit to 0.1 V at a 0.01 V/s scan rate after the cell is equilibrated at the desired conditions.

Results and Discussion

Polynorbornene homopolymer, block copolymer, and random copolymer were synthesized using either bromopropyl norbornene (BPNB) or bromobutyl norbornene (BBNB) as the hydrophilic monomer, which was later quaternized, and butyl norbornene (BuNB) as the

hydrophobic monomer. Scheme 1 shows the synthetic procedure of the three polymers. Gel permeation chromatography (GPC) was used to measure the number average molecular weights (M_n) and dispersity (Đ) of the polymers. The results are reported using a sample number where the numbers represent the mole percent of the hydrophilic monomer in the final polymer product. For example, GT75 is comprised of 75% BBNB and 25% BuNB. The letter "R" is included in the name for the random copolymer architecture. The absence of the letter "R" indicates that it is a block copolymer. The M_n and Đ of the block copolymer (GT75) were 73.80 kDa and 1.51, respectively, random copolymer (GTR75) were 75.63 kDa and 1.16, respectively, and homopolymer (GT100) were 23.31 kDa and 1.42, respectively. Figure 1 shows the GPC traces of the three polymers mentioned above. A schematic representation of the three polymers starting from two different monomers is given below, Scheme 2.

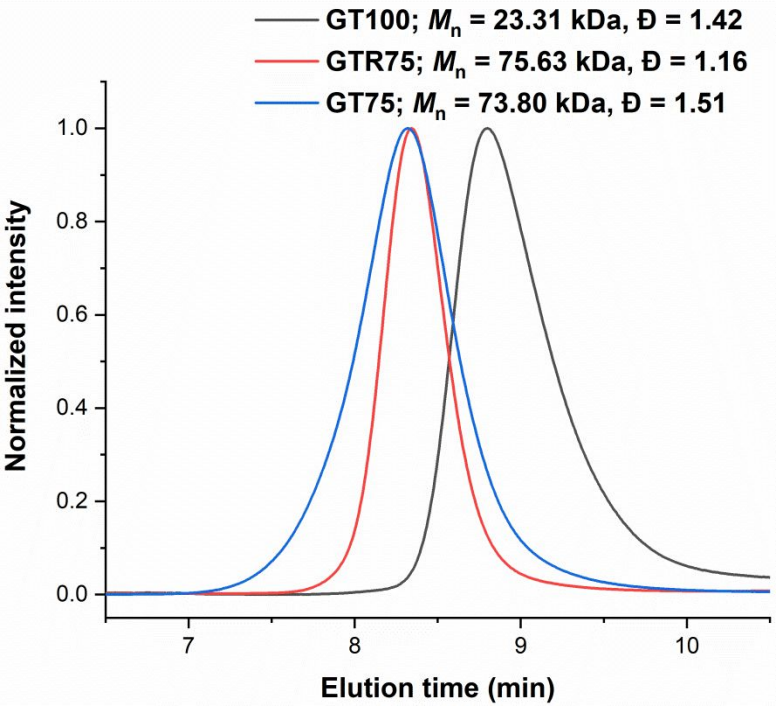

Figure 1. GPC traces of homopolymer, block copolymer, and random copolymers.

A. Homopolymer

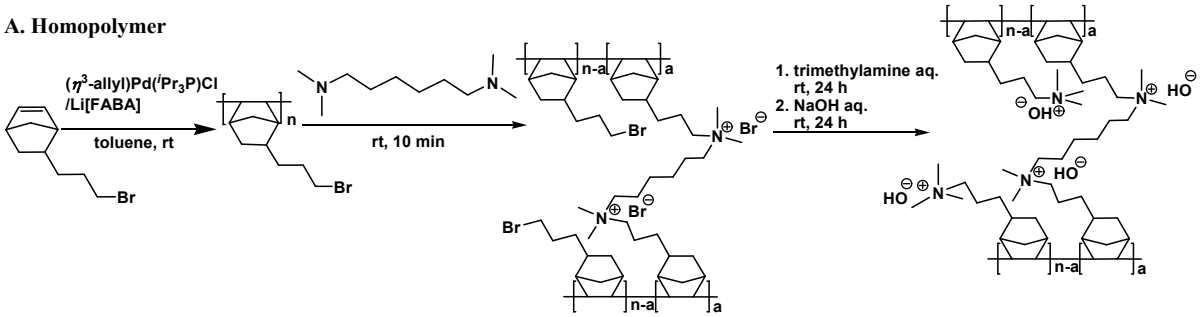

B. Block copolymer

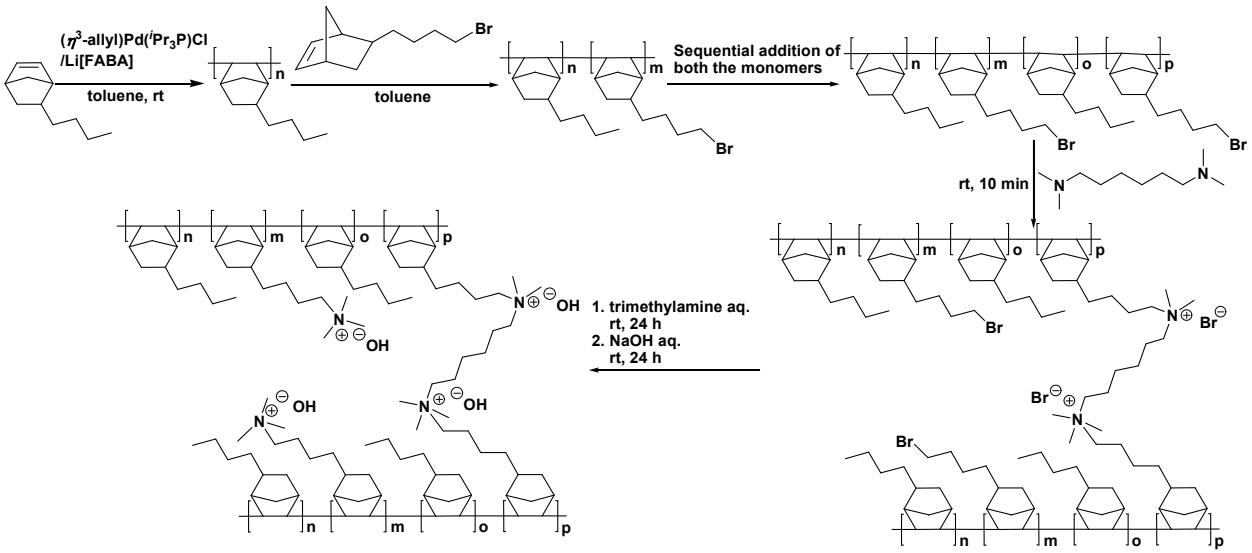

C. Random copolymer

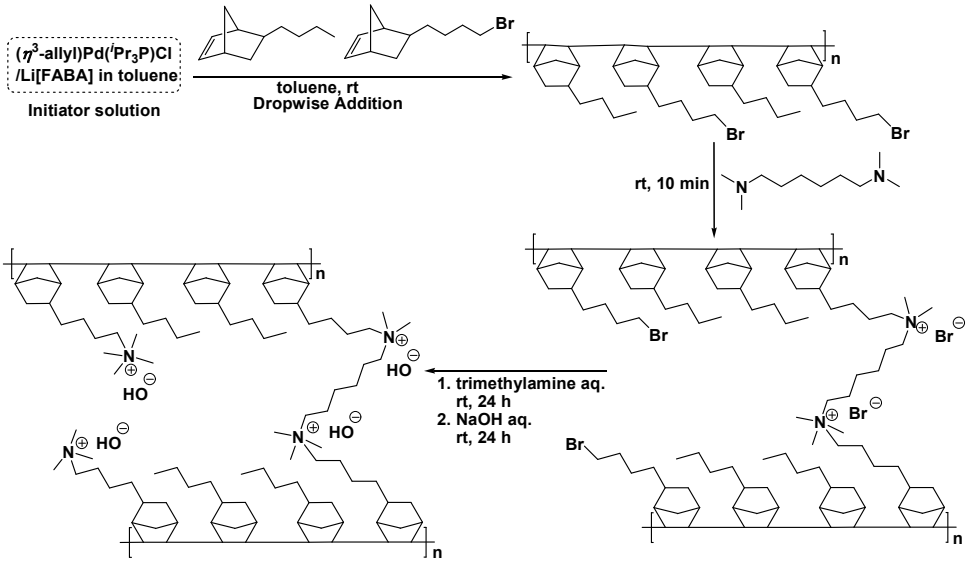

Scheme 1. Synthetic schemes for homopolymer (A), block copolymer (B), and random copolymer (C) for casting the membranes.

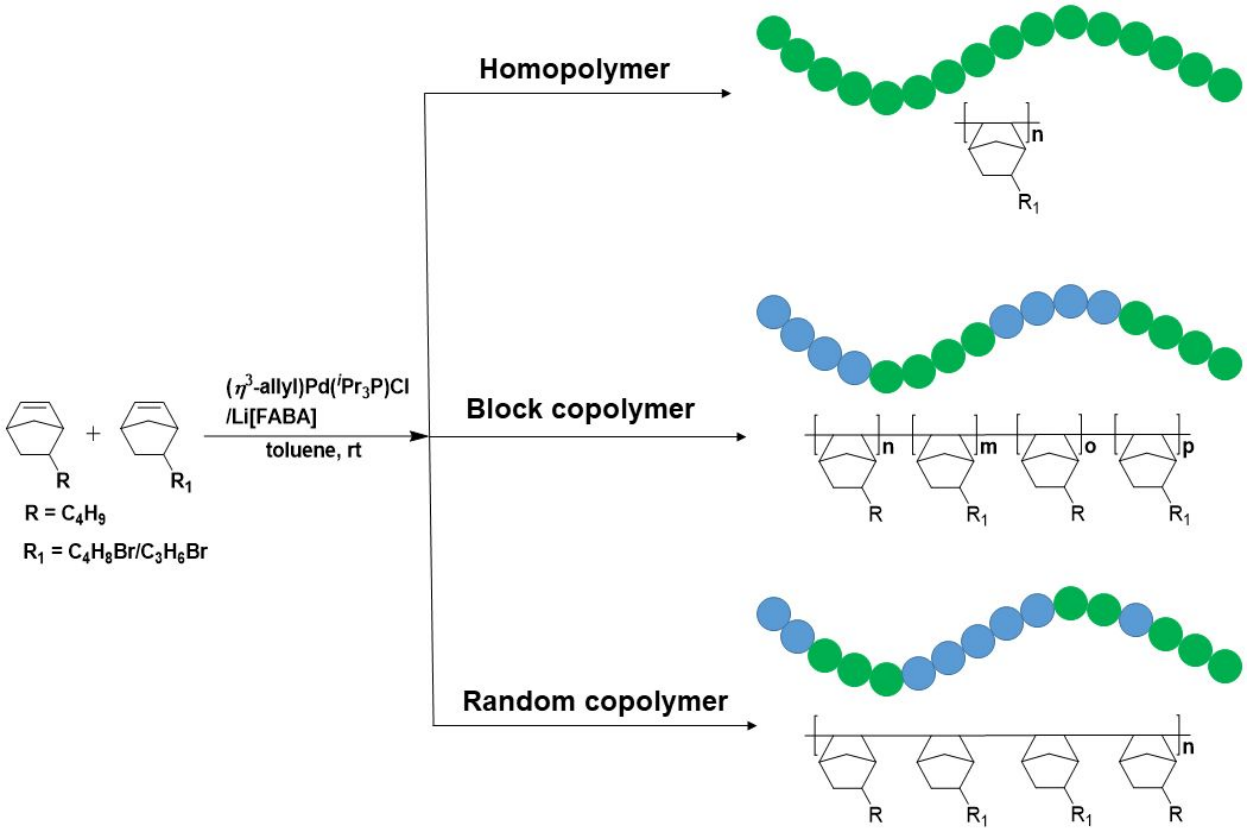

Scheme 2. Synthesis of homopolymer, block copolymer, and random copolymer.

To make freestanding films with the desired mechanical properties, the GT75, GTR75 and GT100 polymers were cross-linked with 5 to 20 mol% TMHDA. The TMHDA concentration is given with respect to the hydrophilic monomer concentration. In the naming convention, the percentage of crosslinker is given after the percent of aminated monomer, separated by a dash. For example, GTR75-10 is a random copolymer with 75 percent halogenated monomer and 10 % TMHDA. It was previously shown that when these films are insufficiently cross-linked (TMHDA concentration less than 5 mol%), the conductivity drops due to the absorption of excessive water in the polymer.[14] Excess water leads to swelling, as well as softening of the membranes and increased brittleness.[14] With no crosslinker, the films immediately gelled when soaked in TMA and the materials could no longer be handled.

The polymers were characterized by ^{1}H NMR to determine the mole ratio of the two monomers in the copolymers and the IECs. The ^{1}H NMR spectra for representative polymers are shown in Figure 2. Additionally, the IECs for all of the cross-linked membranes are reported in Table 1. The final IECs are between 3.48-4.55 meq/g. There is a good correlation between IECs measured by ^{1}H NMR and Mohr's titration method, also shown in Table 1. In the following discussion, block copolymers and random copolymers with similar IEC and M_n, values were chosen for comparison of their physical and electrochemical properties. To confirm the formation of block copolymer and differentiate from random copolymer and homopolymer, morphological characterization by small angle X-ray scattering (SAXS) was performed.

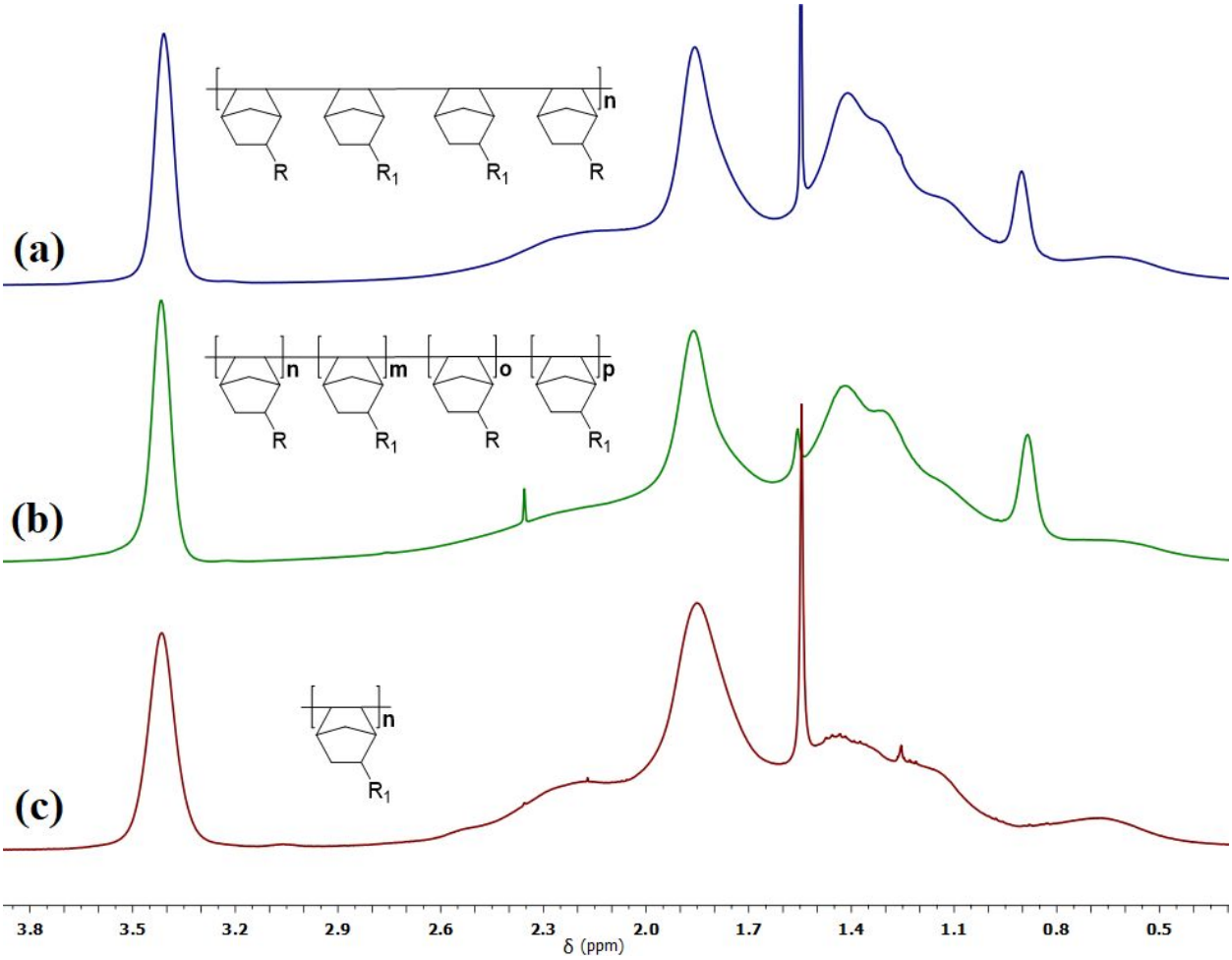

Figure 2. ^{1}H NMR spectra for a (a) random copolymer, (b) block copolymer, and (c) homopolymer in $CDCl_3$.

Table 1 Properties of homopolymer (GT100), block copolymer (GT75), and random copolymer (GTR75) membranes in hydroxide form.

Polymer	TMHDA Concentration (mol%)	OH^- Conductivity (mS/cm)[b]		IEC (meq/g)[c]	IEC (meq/g)[d]	σ/IEC[e]	Ionic ASR[f] (Ohm-cm^2)	Water Uptake[g] (%)	Swelling Volume[g] (%)	Hydration Number[h] (λ)	N_{free}	N_{bound}	*d* spacing *(nm)*
		25 °C	80 °C										
GT100-15[a]	15	66	148	4.55	4.48	32.5	0.06	89	21	10.87	1.73	9.14	NA
GT100-20[a]	20	51	123	4.49	4.39	27.4	0.06	62	12	7.67	0.23	7.44	NA
GT75-5	5	99	201	3.59	3.53	56.0	0.05	119	32	18.42	3.92	14.5	51.9
GT75-15	15	70	155	3.52	3.49	44.0	0.06	66	13	10.42	0.89	9.53	50.0
GTR75-5	5	94	194	3.58	3.50	54.2	0.05	114	31	17.69	8.50	9.19	NA
GTR75-10	10	77	171	3.54	3.48	48.3	0.05	82	19	12.87	3.16	9.71	NA
GTR75-15	15	68	152	3.51	3.47	43.3	0.06	73	16	11.55	3.84	7.71	NA
GTR75-20	20	61	132	3.48	3.40	37.9	0.08	64	12	10.22	1.44	8.82	NA

[a]Homopolymer using bromopropyl norbornene (BPNB) as the halogenated block. [b]OH^- conductivity was measured by four-probe conductivity cell. [c]IEC was determined by ^{1}H NMR. [d]IEC was determined by titration. [e]Ionic conductivity at 80 °C/IEC. [f]Ionic ASR was calculated using the following equation: ASR = L/σ where L = film thickness in cm; σ = ion conductivity in S/cm (at 80 °C). [g]Water uptake and swelling volume were measured at room temperature. Measurements were performed in triplicate to ensure repeatability. The deviation in the measurements of each data point was <3 %. [h]The % error was <4 %.

Small angle X-ray scattering (SAXS) was used to characterize the phase-separated morphology of the block copolymer, random copolymer and homopolymer samples. The primary scattering peak in each SAXS spectra, Figure 3, was used to calculate the Bragg spacing of each sample, which describes the approximate separation length between inhomogeneities within the membranes. Only the block copolymer samples showed distinct scattering peaks. The d-spacing of GT75-5 and GT75-15 were 51.9 nm and 50.0 nm, respectively. The lower TMHDA cross-linker concentration of GT75-5 is expected to allow for higher WU and swelling, discussed later, which is consistent with the slightly larger domain spacing that was observed. The random

copolymer samples lack monomer segments that are long enough to form phase-separated structures and the homopolymer sample inherently lacks a secondary, distinct monomer type. Thus, the primary scattering peaks were not detected in the SAXS spectra for these samples.

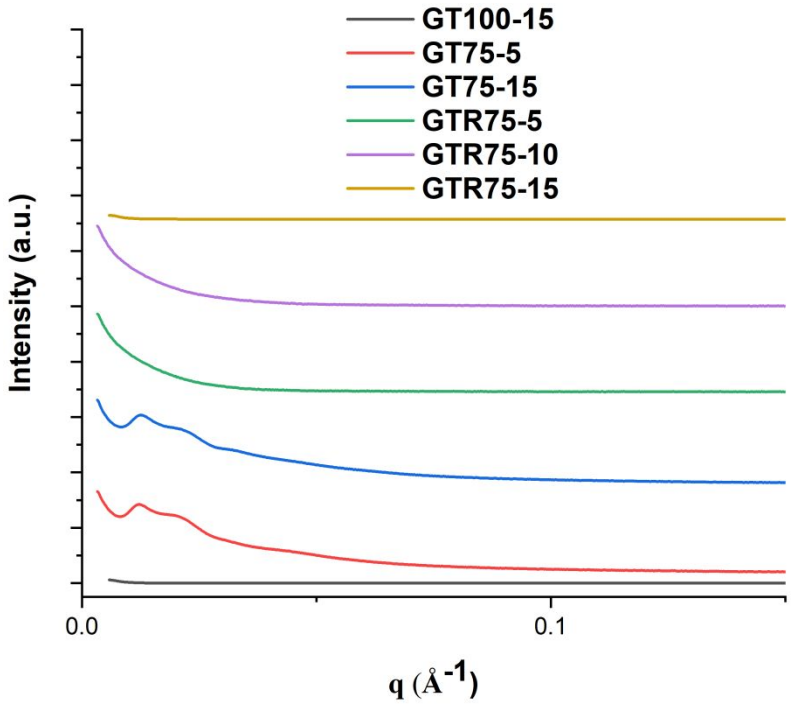

Figure 3. Small angle X-ray scattering spectra of block copolymer (GT75), random copolymer (GTR75) and homopolymer (GT100) membrane samples.

High AEM ionic conductivity is an important factor in electrochemical device fabrication and performance. Figure 4 shows the variation in conductivity with temperature for values between 25 °C and 80 °C. The conductivity increased with temperature due to the higher diffusivity of the ions at elevated temperature. For GT75-5 (block copolymer membrane), the conductivity was 99 mS/cm and 201 mS/cm at 25 °C and 80 °C, respectively. At higher TMHDA concentration, GT75-15, the conductivity was slightly lower, 70 mS/cm and 155 mS/cm at 25 °C and 80 °C, respectively which was due to a reduced amount of water inside the membrane when the membrane was highly cross-linked. For GTR75-5 (random copolymer membrane with 5 mol% TMHDA), the conductivity at 25 °C and 80 °C was 94 mS/cm and 194 mS/cm, respectively. Increasing the TMHDA concentration, (5 mol%, 10 mol%, 15 mol%, 20 mol%) resulted in a drop in the measured conductivity (194 mS/cm, 171 mS/cm, 152 mS/cm,

132 mS/cm, respectively) at 80 °C. The comparable conductivities of GT75-5 (201 mS/cm) and GTR75-5 (194 mS/cm) at 80 °C point toward the suitability of high IEC membranes by cross-linking random copolymers without block copolymer phase segregation. Previously, a systematic comparison of the properties of block and random copolymer AEMs reported by Watanabe et al. showed significantly higher hydroxide conductivity for a multiblock copolymer membrane (126 mS/cm at 60 °C) compared to a random copolymer membrane (35 mS/cm at 60 °C).[34] On the other hand, Coates et al. showed an opposite trend and achieved more than seven times higher (83 mS/cm vs. 11 mS/cm at 80 °C) hydroxide conductivity in random copolymer than block copolymer with similar IECs.[35] The formation of disordered microphase separation in BCP in comparison to homogeneous morphology in random copolymer membrane resulted in a decrease in hydroxide conductivity. Note, in this study, evidence of the formation of block copolymer AEMs were provided by the appearance of distinct SAXS scattering peaks, Figure 3. The cross-linked homopolymer, GT100-15, had a conductivity of 66 mS/cm and 148 mS/cm at 25 °C and 80 °C, respectively. The homopolymers could not be used without cross-linking because it gelled and could not be made into a membrane. At higher cross-linking, GT100-20, the conductivity was much lower, 51 mS/cm and 123 mS/cm at 25 °C and 80 °C, respectively. The ionic conductivity in the cross-linked homopolymer was lower than the random copolymer because the hydroxide mobility dropped. Hence, high IEC homopolymers are not as suitable for AEMs due to lower hydroxide mobility and not because of ion concentration with the membrane. Recently, Jannasch et al. compared the properties of block copolymer AEM and AEM of the same block copolymer after blending with polybenzimidazole (PBI).[36] The researchers showed a 10% and 28% decrease in conductivity and WU, respectively. Moreover, the blended membrane showed higher mechanical robustness than block copolymer membranes without blending with PBI.

The ionic conductivity of the membranes showed an Arrhenius-type temperature dependence between 25 °C and 80 °C. Figure S1 shows the plot of $\ln(\sigma)$ *vs.* 1/T. The apparent activation energies (E_a) were calculated from the slope of the plot and were found to be 11.3 to 14.3 kJ mol^{-1}. This was in agreement with previously reported AEM values.[14,16,37,38] The ionic ASR is a key parameter in electrochemical devices. Table 1 shows the ionic ASR values of all the membranes. The ionic ASR values were as low as 0.05 ohm cm^2, very close to the Department of Energy, USA target metric of ≤0.04 ohm cm^2.

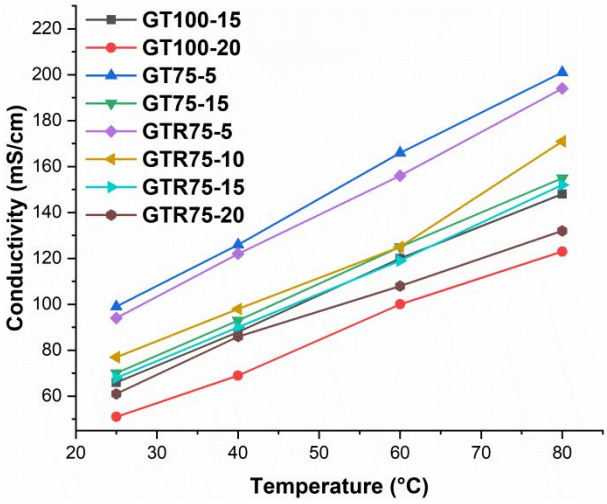

Figure 4. Plot of ionic conductivity of polynorbornene AEMs at different temperatures.

WU plays a key role in hydration and transport of hydroxide ions in AEMs.[39] The WUs of the AEMs are provided in Table 1. With an increase in TMHDA concentration, the WUs decrease. The WUs of GT100-15 and GT100-20 were 89% and 62% respectively, and the conductivities were 148 mS/cm and 123 mS/cm, respectively, at 80 °C. In the case of GT100-5 and GT100-10, the WU for the membranes was 240% and 132%, respectively, and the membranes were brittle and broke into pieces when the TMHDA concentration was >20 mol%. In addition, the lower M_n (23.31 kDa) of GT100-X made the membranes mechanically weak. Hence, it was not possible to collect more data with the GT100 sample. For GT75 AEMs, the WU was 119% and 66% at 5 mol% and 15 mol% TMHDA concentration, respectively. The WU decreased from 114% to 64% for GTR75-X when the TMHDA concentration increased from 5 mol% to 20 mol% (i.e., GT75-5 to GT75-20). The conductivity followed the same trend as WU and decreased from 194 mS/cm to 132 mS/cm at 80 °C due to the lower number water for hydration and transport of ions. For GT75 and GTR75 with similar M_n and IEC values, the WU was comparable at 5 mol% (119% for GT75-5 *vs.* 114% for GTR75-5) and 15 mol% (66% for GT75-5 *vs.* 64% for GTR75-5) TMHDA concentration. Note that the WU of the uncross-linked GTR75 membrane was 1190% making it impossible to carry out additional measurements. The

hydration number (λ) is a measure of number of water molecules per ammonium group. Like WU, λ also decreased with an increase in TMHDA concentration. For example, λ of GTR75 membranes decreased from 17.69 to 10.22 when the TMHDA concentration increased from 5 mol% to 20 mol%. The comparable WU, λ, and conductivity values of GT75 and GTR75 AEMs indicated that the formation of more complex block copolymer AEMs in comparison to random copolymer AEMs is not practically needed if random copolymer AEMs are made with sufficient IECs and managing water properly inside the membrane. This is further confirmed by the comparable device performances of GT75 and GTR75 composite membranes, discussed below.

DSC was used to calculate the number of non-freezable or bound (N_{bound}) and unbound or freezable (N_{free}) from λ. N_{free} helps in the transport of ions, however excess N_{free} can flood the ion conducting channel and conductivity drops. N_{bound} helps in the hydration of ions. Hence, an optimum amount of N_{free} and N_{bound} is necessary for maximum hydroxide mobility and water transport. The current study shows a decrease in ionic conductivity when there is an insufficient amount of N_{free} and N_{bound}. For example, the conductivity of GTR75-5 and GTR75-15 membranes dropped from 194 mS/cm to 132 mS/cm at 80 °C, respectively when the N_{free} decreased from 8.5 to 1.4, Table 1. Similar conclusion can be drawn for GT100 and GT75 membranes.

The random and block copolymers were chosen (same IEC and M_n) in such a way that IEC and M_n of both the polymers don't influence the mechanical properties. The storage modulus of the membranes from random and block copolymer showed no practical difference in mechanical properties. For example, the storage modulus of GT75-15 and GTR75-15 was 0.63 MPa and 0.54 MPa, respectively.

Another important consideration for AEMs is their long-term chemical stability, which can be translated to longer life for alkaline electrochemical devices, such as fuel cells and electrolyzers. To determine the alkaline stability, each type of membrane was immersed in 1 M NaOH solution at 80 °C and the drop in ionic conductivity was monitored for >1000 h, as shown in Figure 5. The membranes had <1.35% drop in conductivity regardless of the architecture. This finding is consistent with previous results.[13-16] AEMs made from polymers with an all-hydrocarbon backbone and the tethered cations (long alkyl chain) have shown exceptional chemical stability. Evidence of intact chemical structure after alkaline aging was shown in a previous study using FT-IR spectroscopy .[14-16]

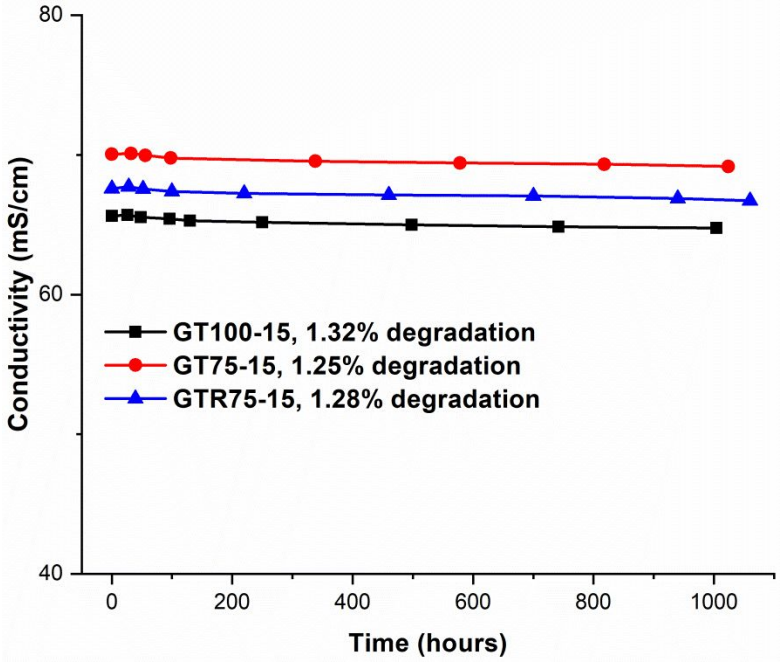

Figure 5. Alkaline stability analysis of homopolymer, block copolymer, and random copolymer membranes in 1 M NaOH solution at 80 °C.

Previous results showed excellent H_2/O_2 fuel cell performance with thin, composite block copolymer poly(norbornene) membranes.[16,17] In this study, block copolymer and random copolymer AEMs were tested with similar electrodes and operating conditions. During this hydration and ion exchange process, the MEAs remained intact which indicates adequate adhesion of the catalyst layer within the MEA. The electrodes were identical to those published previously.[16,17] For both cases, GT73 ionomer was used for anode electrode and GT32 ionomer was used in cathode electrode. Multiple cells were assembled to ensure repeatability. Polarization curves were collected with H_2/O_2 feed gases, fed at a volumetric flow rate of 1 L/min, and the results are shown in Figure 6.

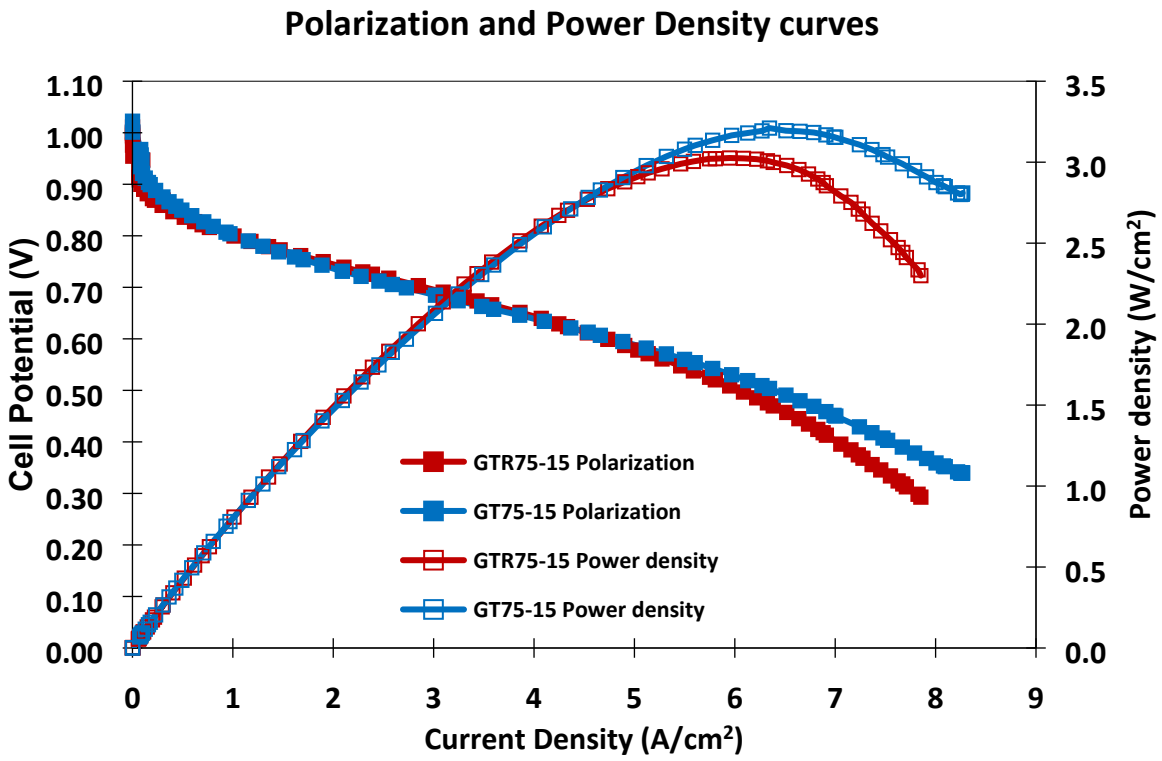

Figure 6. Current-voltage (filled) and current-power density (empty) curves for AEMFCs with a 10 µm GTR75-15 AEM, operating with H_2/O_2 (Red) and 10 µm GT75-15 AEM, operating with H_2/O_2 (Blue), feeds at 1 L/min. The cell temperature was 80 ºC. The anode/cathode dew points were optimized at 70 ºC/74 ºC for GTR75-15 and 68 ºC/70 ºC, for GT75-15. The actual anode loading was 0.672 $mg_{Pt/Ru}$ cm^{-2} and for cathode was 0.584 mg_{Pt} cm^{-2}, with no backpressure.

A peak power density of 3.21 W/cm^2 and a maximum current density of 8.27 A/cm^2 polarized up to 0.3 V at 80 °C with H_2/O_2 was achieved in case of GT75-15 membrane. The peak power density was 3.05 W/cm^2 and the maximum current density was 7.85 A/cm^2 at 80°C with H_2/O_2 using the GTR75-15 membrane. Gerhardt *et al.* have shown that the rate of water transport from anode towards cathode is the current-limiting factor in AEM fuel cells.[25] An average high frequency resistance (HFR) of ca. 5 mOhm was observed which shows that both types of membrane have low internal resistance in the cell. The polarization curves for both membrane overlap each other in the low current region (kinetic and ohmic region), however, the GTR75-15 membrane had slightly lower performance in the high-current, mass transport region. This high performance was due to a combination of factors including high ionic conductivity (i.e. low internal resistance loss), low membrane and ionomer WU and high water transport through the AEM from the hydrogen anode to the oxygen cathode during operation. This suggests that random copolymer membranes are suitable for high performance fuel cell devices, as long as the

IEC is high. This is an important finding because the use of random copolymer membranes simplifies the manufacturing process and lowers cost compared to block copolymer membranes. This study shows that random copolymer AEMs can be suitable for electrochemical devices if they have very high IEC, incorporate a low concentration of cross-linker to mitigate excess WU and swelling. It was also shown that these polymers can be formed into very thin membranes for enhanced water management during cell operation.

Conclusions

The synthesis and characterization of different AEMs using polynorbornene homopolymer, block copolymer, and random copolymer has been demonstrated. The IECs were in the range between 3.48-4.55 meq/g. The membranes were cast after cross-linking with TMHDA to mitigate the penalty of excess WU due to high IECs. The morphological characterization showed phase segregation in block copolymer whereas, no phase separation was observed in the homopolymer and random copolymer. The conductivities of GTR75-5 (random copolymer) and GT75-5 (block copolymer) samples were comparable (194 mS/cm *vs.* 201 mS/cm, respectively, at 80 °C) and indicates that phase-segregated morphology is not essential to achieve high conductivity. The membranes were base-stable and showed <1.35% loss of conductivity after 1000 h aging in NaOH at 80 °C. For GTR75-15 sample, the peak power density of 3.05 mW/cm^2 in a H_2/O_2 fuel cell at 80 °C showed the suitability of random copolymers in electrochemical devices.

Acknowledgement: GT gratefully acknowledge the discussions and support from Larry Rhodes, Doug Skilskyj and Matt Barchok at Promerus LLC, and the financial support of the ARPA-E IONICS program. USC would like to acknowledge the financial support of the U.S. Department of Energy Office of Energy Efficiency & Renewable Energy (award number Award Number: DE- EE0008433). The authors also acknowledge the support of Jong Keum of Oak Ridge National Laboratory for the performance of the SAXS measurements.

References

1. J. R. Varcoe, P. Atanassov, D. R. Dekel, A. M. Herring, M. A. Hickner, P. A. Kohl, A. R. Kucernak, W. E. Mustain, K. Nijmeijer, K. Scott, T. W. Xu and L. Zhuang, *Energy Environ. Sci.*, 2014, **7**, 3135-3191.

2. L. Carrette, K. A. Friedrich and U. Stimming, *Fuel Cells*, 2001, **1**, 5-39.

3. M. Winter and R. J. Brodd, *Chem. Rev.*, 2004, **104**, 4245-4270.

4. B. C. H. Steele and A. Heinzel, *Nature*, 2001, **414**, 345-352.

5. S. Lu, J. Pan, A. Huang, L. Zhuang and J. Lu, *Proc. Natl. Acad. Sci. U. S. A.*, 2008, **105**, 20611-20614.

6. E. H. Yu, X. Wang, U. Krewer, L. Li and K. Scott, *Energy Environ. Sci.*, 2012, **5**, 5668-5680.

7. M. A. Hickner, A. M. Herring and E. B. Coughlin, *J. Polym. Sci., Part B: Polym. Phys.*, 2013, **51**, 1727-1735.

8. J. Zhou, K. Joseph, J. M. Ahlfield, D.-Y. Park and P. A. Kohl, *J. Electrochem. Soc.*, 2013, **160**, F1648-F1653.

9. C. G. Arges and L. Zhang, *ACS Appl. Energy Mater.*, 2018, **1**, 2991-3012.

10. A. D. Mohanty and C. Bae, *J. Mater. Chem. A*, 2014, **2**, 17314-17320.

11. L. Liu, J. Ahlfield, A. Tricker, D. Chu and P. A. Kohl, *J. Mater. Chem. A*, 2016, **4**, 16233-16244.

12. A. D. Mohanty, S. E. Tignor, M. R. Sturgeon, H. Long, B. S. Pivovar and C. Bae, *J. Electrochem. Soc.*, 2017, **164**, F1279-F1285.

13. M. Mandal, G. Huang and P. A. Kohl, *J. Membr. Sci.*, 2019, **570−571**, 394-402.

14. M. Mandal, G. Huang and P. A. Kohl, *ACS Appl. Energy Mater.*, 2019, **2**, 2447-2457.

15. W. Chen, M. Mandal, G. Huang, X. Wu, G. He and P. A. Kohl, *ACS Appl. Energy Mater.*, 2019, **2**, 2458-2468.

16. M. Mandal, G. Huang, N. U. Hassan, X. Peng, T. Gu, A. H. Brooks-Starks, B. Bahar, W. E. Mustain and P. A. Kohl, *J. Electrochem. Soc.*, 2020, **167,** 054501**.**

17. G. Huang, M. Mandal, X. Peng, A. C. Yang-Neyerlin, B. S. Pivovar, W. E. Mustain and P. A. Kohl, *J. Electrochem. Soc.*, 2019, **166**, F637- F644.

18. Z. Wang, M. Mandal, S. Sankarasubramanian, G. Huang, P. A. Kohl and V. K. Ramani, *ACS Appl. Energy Mater.*, 2020, **3**, 4449-4456.

19. L. Liu, G. Huang and P. A. Kohl, *J. Mater. Chem. A*, 2018, **6**, 9000-9008.

20. W.-H. Lee, E. J. Park, J. Han, D. W. Shin, Y. S. Kim and C. Bae, *ACS Macro Lett.*, 2017, **6**, 566-570.

21. H.-S. Dang and P. Jannasch, *J. Mater. Chem. A*, 2016, **4**, 11924-11938.

22. A. M. A. Mahmoud and K. Miyatake, *J. Mater. Chem. A*, 2018, **6**, 14400-14409.

23. T. J. Omasta, A. M. Park, J. M. LaManna, Y. Zhang, X. Peng, L. Wang, D. L. Jacobson, J. R. Varcoe, D. S. Hussey, B. S. Pivovar and W. E. Mustain, *Energy Environ. Sci.*, 2018, **11**, 551-558.

24. T. J. Omasta, L. Wang, X. Peng, C. A. Lewis, J. R. Varcoe and W. E. Mustain, *J. Power Sources*, 2018, **375**, 205-213.

25. M. R. Gerhardt, L. M. Pant and A. Z. Weber, *J. Electrochem. Soc.*, 2019, **166**, F3180- F3192.

26. X. Gao, H. Yu, B. Qin, J. Jia, J. Hao, F. Xie and Z. Shao, *Polym. Chem.*, 2019, **10**, 1894-1903.

27. J. Lipian, R. A. Mimna, J. C. Fondran, D. Yandulov, R. A. Shick, B. L. Goodall, L. F. Rhodes and J. C. Huffman, *Macromolecules*, 2002, **35**, 8969-8977.

28. D.-G. Kim, T. Takigawa, T. Kashino, O. Burtovyy, A. Bell and R. A. Register, *Chem. Mater.*, 2015, **27**, 6791-6801.

29. C. Wang, B. Mo, Z. He, Q. Shao, D. Pan, E. Wujick, J. Guo, X. Xie, X. Xie and Z. Guo, *J. Membr. Sci.*, 2018, **556**, 118-125.

30. S. J. Lue and S. J. Shieh, *J. Macromol. Sci. Part B: Phys.*, 2009, **48**, 114-127.

31. B. Mecheri, V. Felice, Z. Zhang, A. D'Epifanio, S. Licoccia and A. C. Tavares, *J. Phys. Chem. C*, 2012, **116**, 20820-20829.

32. A. L. Moster and B. S. Mitchell, *J. Appl. Polym. Sci.*, 2009, **113**, 243-250.

33. L. Wang, X. Peng, W. E. Mustain and J. R. Varcoe, *Energy Environ. Sci.*, 2019, **12**, 1575-1579.

34. M. Tanaka, K. Fukasawa, E. Nishino, S. Yamaguchi, K. Yamada, H. Tanaka, B. Bae, K. Miyatake and M. Watanabe, *J. Am. Chem. Soc.*, 2011, **133**, 10646-10654.

35. W. You, E. Padgett, S. N. MacMillan, D. A. Muller and G. W. Coates, *Proc. Natl. Acad. Sci. U. S. A.*, 2019, 116, 9729-9734.

36. J. S. Olsson, T. H. Pham and P. Jannasch, *Macromolecules*, 2020, **53**, 4722-4732.

37. X. Ren, S. C. Price, A. C. Jackson, N. Pomerantz and F. L. Beyer, *ACS Appl. Mater. Interfaces*, 2014, **6**, 13330-13333.

38. H. Ono, J. Miyake, S. Shimada, M. Uchida and K. Miyatake, *J. Mater. Chem. A*, 2015, **3**, 21779-21788.

39. J. Pan, S. Lu, Y. Li, A. Huang, L. Zhuang and J. Lu, *Adv. Funct. Mater.*, 2010, **20**, 312-319.

TOC

A systematic comparison between random and block copolymer membrane properties showed the suitability of random copolymer membranes.